University of Groningen

Interactions between Emiliania huxleyi and the dissolved inorganic carbon system

Buitenhuis, Erik Theodoor

IMPORTANT NOTE: You are advised to consult the publisher's version (publisher's PDF) if you wish to cite from it. Please check the document version below.

Document Version
Publisher's PDF, also known as Version of record

Publication date:
2000

[Link to publication in University of Groningen/UMCG research database](#)

Chapter 5: Blooms of *Emiliania huxleyi* are sinks of atmospheric carbon dioxide; a field and mesocosm study derived simulation.

Erik T. Buitenhuis, Paul van der Wal, Hein J. W. de Baar.

Abstract

During field measurements in a bloom of *Emiliania huxleyi* in the North Sea in 1993, an apparently inconsistent combination of observations was measured:

a) fCO_2 was lower in the centre of the bloom than in the surrounding non-bloom areas, and undersaturated with respect to the atmosphere in both cases,

b) within the bloom enhanced sedimentation of coccoliths-containing fecal pellets was observed,

c) a large atmospheric sink of 1.3 mol $C \cdot m^{-2}$ was derived,

d) in the same bloom a positive correlation between $CaCO_3$ and fCO_2 was observed, which was interpreted as an increase of fCO_2 during production of $CaCO_3$.

In order to resolve the inconsistency between observations (a, b, c) and d a one-dimensional three-layer model was constructed. A positive correlation between $CaCO_3$ and fCO_2 was obtained when the model was parameterised with data obtained from field and mesocosm studies. The correlation is a feature of the decay-phase of a bloom, and represents a decrease of fCO_2 with a decrease of $CaCO_3$. Thus it represents the dissolution and sedimentation of $CaCO_3$ rather than its production. Having resolved the ambiguity within the field data by adding the dimension of time in the model, blooms of *E. huxleyi* can be identified as sinks for atmospheric carbon dioxide. This sink is a function of the calcification to photosynthesis (C:P) ratio of the nitrate-using phytoplankton, and is maximal when the C:P ratio is 0.42 (that is, *E. huxleyi* constitutes 97% of the nitrate-using phytoplankton). Rather than using the model for making accurate predictions about the magnitude of this sink a sensitivity analysis was performed to give a range of magnitudes for the range of parameter values that were obtained during previous studies. Furthermore gaps were identified in the current knowledge of carbon fluxes within blooms of *E. huxleyi*.

Key words: air-sea gas exchange, calcification, calcite ($CaCO_3$), carbon dioxide (CO_2), carbon flux, coccolithophorid, Prymnesiophyceae, sedimentation.

Introduction

Calcification (precipitation of $CaCO_3$) decreases alkalinity twice as much as dissolved inorganic carbon (DIC). As the chemical speciation of DIC in seawater has been accurately determined (Millero 1995), it follows that the fugacity of CO_2 (fCO_2) increases. However, calcification by *Emiliania huxleyi* is at least loosely coupled to photosynthesis, which decreases DIC and has a smaller effect on alkalinity. Alkalinity increases during uptake of nitrate (NO_3^-) and phosphate (HPO_4^{2-}), and decreases during uptake of ammonia (NH_4^+). The combined effect of calcification (C) and photosynthesis (P), then, results in a decrease of fCO_2 at C:P production ratios lower than 1.7 during use of nitrate (C:P < 1.2 during use of ammonia), and an increase of fCO_2 at higher C:P production ratios. Blooms of *Emiliania huxleyi* have therefore been suggested as potential sources of CO_2 for the atmosphere. Robertson et al. (1994) concluded that blooms of *E. huxleyi* may constitute smaller sinks than blooms of non-calcifying algae. This conclusion was based on observations in the North Atlantic Ocean, where fCO_2 was 15 µatm. higher in samples with $CaCO_3$ > 18 µM than in samples with $CaCO_3$ < 5.5 µM. Crawford & Purdie (1997) calculated an actual increase of fCO_2 in blooms of *E. huxleyi*, but this was

found under the extreme conditions of 100% mineralisation of POC and 0% dissolution of $CaCO_3$.

Wal et al. (1995) found that sedimentation of carbon is enhanced in a bloom of *E. huxleyi* due to the increased weight of fecal pellets that contain coccoliths. This physical effect of enhanced sedimentation complicates the above mentioned chemical effect of calcification on alkalinity, and thereby on fCO_2. Sedimentation of particulate carbon itself will not change the air-sea gradient of CO_2. However, if the carbon remains suspended in the surface waters, then it will eventually be mineralized again and the end result will be no different from the situation before the start of the bloom, while any material that is sedimented below the thermocline will leave the surface waters undersaturated for carbon dioxide.

To illustrate this point first a model is considered with two boxes: atmosphere and surface water. This model simulates a bloom with first production and then degradation of both particulate organic carbon (POC) and calcite ($CaCO_3$). If the C:P production ratio in the model is lower than 1.7 then during the productive stage CO_2 will decrease and gas exchange will transport CO_2 from the atmosphere to the sea. During the degradation stage CO_2 will increase and CO_2 will outgas from the sea to the atmosphere. At the end of the bloom the situation will be the same as at the start, so that the net exchange with the atmosphere will be zero.

This two box model can be used to illustrate the chemical effect of calcite production. To include the physical effect of calcite in sinking particles a third box is introduced: the deep sea. The same hypothetical model simulation can now be performed with a bloom in the upper ocean, which is later degraded, and some material being transported to the deep layer. Since exchange of dissolved constituents (DIC, alkalinity etc.) between the upper and the deep layer is slow relative to the production and degradation of the bloom, by the end of the bloom the effect of gas exchange with the atmosphere will be a function of the amount of POC and $CaCO_3$ that is sedimented to the deep layer. The more POC and the less $CaCO_3$ is sedimented the more CO_2 will be drawn down from the atmosphere. But if the amount of sedimented POC is stimulated by the amount of heavy $CaCO_3$ in the sedimenting particles then $CaCO_3$ both reduces and increases CO_2 drawdown from the atmosphere. Thus, it has to be determined whether the chemical effect of $CaCO_3$ precipitation is more or less important than the physical effect of $CaCO_3$ enhancing sedimentation. This was done by constructing a three box model using data from several studies of blooms of *E. huxleyi*.

The model that is presented here includes those processes that were found to occur during both a natural bloom of *E. huxleyi* in the North Sea in 1993 (Wal et al. 1995, Buitenhuis et al. 1996, Wiebinga et al. 2000) and a mesocosm study at the field station of the University of Bergen in Raunefjord in 1992 (Bleijswijk et al. 1994a, Wal et al. 1994, Bleijswijk & Veldhuis 1995). Parameter values were also taken from these studies.

Model description

The model simulates an algal bloom within a 1-D sea with three boxes: an atmosphere with constant fCO_2, a mixed layer with a constant depth of 40 m and a deep layer of 80 m depth. The model contains 7 carbon pools, three nitrogen pools, two pools of alkalinity, and a fixed atmospheric fCO_2 (Figure 5.1). All simulations were run for 60 days with a variable time step to minimize integration errors. Cumulative integration errors were always less than 10^{-12} of the total pools. Most of the parameter values, and some of their ranges for the sensitivity analysis were taken from a field study in the North Sea in 1993 (Wal et al. 1995, Buitenhuis et al. 1996, Wiebinga et al. 2000) and a mesocosm study in Raunefjorden, Norway in 1992 (Bleijswijk et al. 1994a, Wal et al. 1994, Bleijswijk & Veldhuis 1995). Additional parameter values were taken or derived from Redfield et al. (1963), Alldredge & Gotschalk (1988), Bleijswijk et al. (1991, 1994b), Wanninkhof (1992), Chipman et al. (1993), Roy et al. (1993) and Buitenhuis et al. (1999).
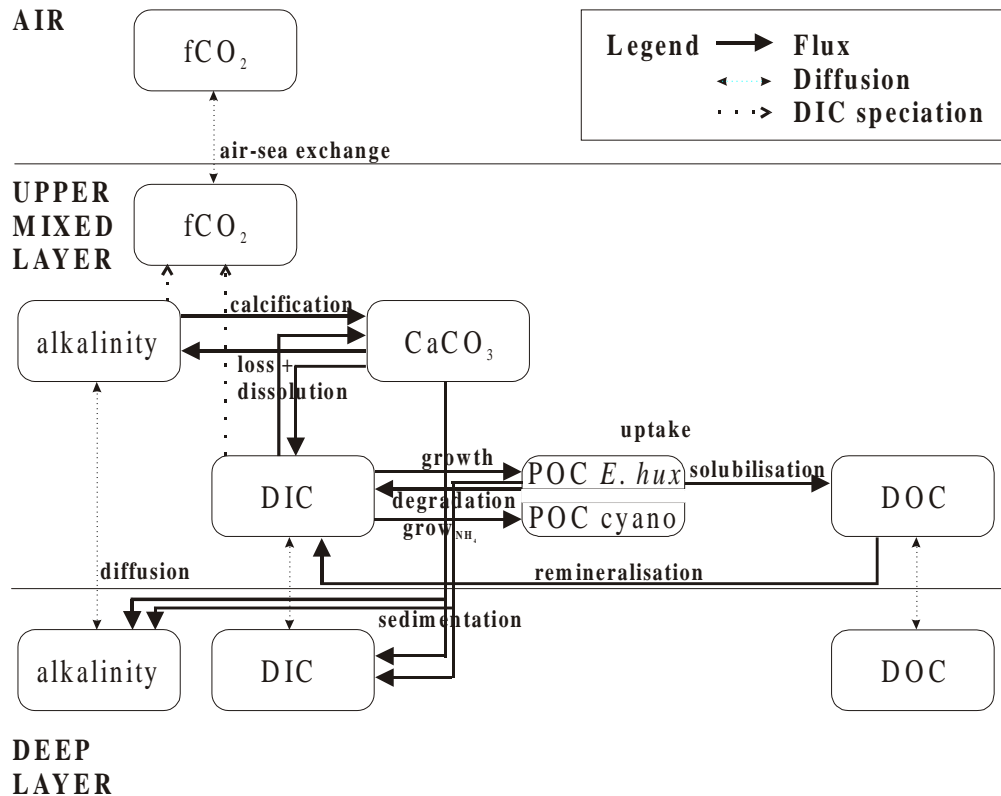
Figure 5.1 Simplified scheme of the model structure. Pools and fluxes of nitrogen and feedback controls have been omitted. Dotted arrows of DIC speciation indicate that fCO_2 was calculated from DIC and alkalinity (see the 'CO₂fromDIC,alkalinity' function in section 2.8 for details). Air-sea gas exchange was added to DIC.

Model structure

The model structure is shown in Figure 5.1, and is described from top to bottom and from left to right.

The air has a constant fCO_2 of 360 µatm. In the upper mixed layer fCO_2 is calculated from alkalinity and DIC with the dissociation constants of Roy et al. (1993). The starting values of alkalinity and DIC were chosen in such a way that the fCO_2 at the start of the model run was 360 µatm. at a temperature of 11.6 °C and a salinity of 35.2.

The calcification rate (C) is proportional (C:P parameter) to the growth rate (or photosynthesis P), but with a delay. At the start of the model runs, for the length of the delay period, the C:P production ratio is equal to the C:P parameter. After that the C:P production ratio becomes slightly higher than the C:P parameter, until it becomes close to infinite as the NO_3^- concentration approaches 0. The C:P production ratio stays very high for the length of the delay period, after which both calcification and photosynthesis are very small for the remainder of the model run. The delay is introduced because calcification continues after photosynthesis becomes nutrient-limited. In cultures, this delay was 2 to 3 days (Dong et al. 1993, Paasche 1998). In the mesocosm study calcification rates were still 41 % of the average rates four days after the peaks of *E. huxleyi* (Wal et al. 1994), possibly because nutrients were added daily

during this study. Even so, the standing stock of $CaCO_3$ also went through a distinct maximum two days after the peak in POC was reached (Bleijswijk et al. 1994a).

The sedimentation rate is proportional to the sinking rate, calculated with Stokes' law (see the SEDIMENTATION function in the Materials & Methods section This is consistent with the observation that fecal pellets that contain $CaCO_3$ sink rapidly out of the upper mixed layer, whereas fecal pellets without $CaCO_3$ stay suspended in the upper mixed layer for longer periods, and are more prone to be degraded there (Wal et al. 1995).

The net growth rate is composed of a gross growth rate and loss factors (Bleijswijk et al. 1995). The gross growth rate is a function of nitrate (NO_3^-) according to Michaelis-Menten kinetics (Michaelis & Menten 1913). The loss rate is composed of sedimentation, solubilisation (to DOC) and degradation (to DIC). The declining phase of the bloom is then brought about by nutrient limitation of the gross growth rate, and a loss rate that continues unabated.

The standard model calculates only the C-fluxes due to *E. huxleyi*. In reality, the new production of *E. huxleyi* is followed by a secondary growth of cyanobacteria (Buitenhuis et al. 1996). In one of the runs of the sensitivity analysis an additional component (POC_{cyano}) was introduced to represent the C-flux associated with this secondary growth. In the model *E. huxleyi* uses only nitrate, while the cyanobacteria use only ammonia. This is a simplification of the observation that new production tends to depend mostly on nitrate, while recycled production uses mostly ammonia. It was chosen as a simple means of representing the complex factors that lead to bloom formation, rather than as a representation of the real situation (which is presented in Stolte 1996). The total primary production was found to be fairly constant throughout the bloom (Wal et al. 1995). Thus, the secondary growth appears to be a recycling pool of carbon, and therefore mineralisation and sedimentation of this pool are not included.

Diffusive exchange of dissolved constituents between the upper mixed layer and the deep layer is calculated as due to turbulent mixing. Water exchange by variations in the mixed layer depth were not included. For our objective of unraveling general trends an average wind speed was most suitable. When attempting to simulate a specific bloom, variations in the wind speed can have a large influence (see also 4.1 in the discussion and *Bakker et al.* [1997]).

Parameter values

The processes are described from top to bottom and from left to right as well (Figure 5.1).

The exchange rate between fCO_2 in the air and the upper mixed layer was calculated on the basis of the equation for average wind speeds given by Wanninkhof (1992) using the observed average wind speed of 7.2 $m \cdot s^{-1}$ (Buitenhuis et al. 1996). The sum of this exchange is presented as the air-sea flux. At the end of each model run all particulate and organic carbon in the upper mixed layer is mineralised and the flux of CO_2 is calculated to bring the upper mixed layer in equilibrium with the atmosphere. This is added to the air-sea flux during the model run. The results of this flux are presented as the potential flux. Thus, the potential flux is the effect of sedimentation and diffusive exchange between the upper mixed layer and the deep layer, expressed in units of mol $CO_2 \cdot m^{-2}$.

The C:P parameter was calculated as 0.433, based on 20 coccoliths$\cdot$cell^{-1} of 21.7 fmol $CaCO_3 \cdot$coccoliths^{-1} per 1 pmol POC$\cdot$cell^{-1} (Wal et al. 1994, Buitenhuis et al. 1999).

Dissolution of newly produced coccoliths was undetectable for the first 2 days (Wal et al. 1995), but on the other hand the dissolution rate during the end phase of a bloom was 25 % per day (Buitenhuis et al. 1996). About 75 % of the coccoliths of a cell were dissolved during loss of a cell (Bleijswijk et al 1994a). In an attempt to combine these observations, dissolution of $CaCO_3$ was composed of two components. During the growth phase of the bloom dissolution is associated by a 75% loss parameter with the three loss factors (sedimentation, solubilisation and degradation). Additionally, during the declining phase of the bloom 17 % of the standing stock of $CaCO_3$ dissolves per day, to bring the total dissolution rate to 25% per day.

Nitrate was set at 6 µM at the start of the model run, which was the concentration to the north of the North Sea bloom (Veldhuis 1993). Nitrate is taken up by $POC_{E.hux}$ with a C:N ratio of 7.4 (Buitenhuis et al. 1999) Ammonia is taken up by POC_{cyano} with a C:N ratio of 6.625 (Redfield et al. 1963). For both nutrients the $K_{1/2}$ was 0.1 µM. The effect of uptake and excretion of nitrate, ammonia and phosphate (N:P = 16) on alkalinity was included in the model.

The sedimentation function was based on Stokes´ law. In the sensitivity analysis the value of power was -1.32 and -1.08 to give the same total sedimented fluxes as calculated with fixed sedimentation rates of 0.02 and 0.12 d^{-1} (Wal et al.1995). In the standard run power was set at -1.2. For details, see the description of the SEDIMENTATION function in the Materials & Methods section.

A gross growth rate of 0.69 d^{-1} is based on measurements during the growing phase in a mesocosm study (Bleijswijk & Veldhuis 1995). A solubilisation rate of 0.06 d^{-1} was chosen to give rise to a production of DOC of 0.6 mol·m^{-2} (Wiebinga et al. 2000). A degradation rate of 0.07 d^{-1} was used to give a total loss rate of 0.2 d^{-1} (Bleijswijk & Veldhuis 1995).

DOC is a composite of different molecules with differing biodegradabilities. For practical purposes DOC can be subdivided into three pools. The most labile fraction is degraded almost as fast as it is produced (viewed on a daily basis). The second fraction can accumulate during algal blooms, but is located in the upper mixed layer of these high productivity areas, and is thus degraded over timescales at which water transport takes place. The most refractory fraction is degraded only very slowly, and can be found as a constant concentration in the deep ocean, and as the background to the more labile pools in the upper ocean (cf. Wiebinga 1999) The first and last pools have turnover times that fall outside of the scope of this model, and the DOC pool in the model represents only the intermediately refractory fraction. A comparison of DOC profiles taken during different stages of the North Sea bloom of *Emiliania huxleyi* has shown that DOC increases up to the peak of the bloom to a concentration of 0.6 mol·m^{-2}. The degradation rate was not fast enough to be detectable (Wiebinga et al. 2000). A low remineralisation rate of 0.003 d^{-1} (which gives a half life of 230 days) was used in the standard model, and a rate of 0.03 d^{-1} (which gives a half life of 23 days) in the sensitivity analysis.

Vertical diffusivities in stratified water vary between approximately 10^{-5} and 10^{-4} m^2·s^{-1} (Chipman et al. 1993). Since blooms of *E. huxleyi* are normally observed in stable water columns the lower diffusivity was used in the standard model run, and the higher of the two was used in the sensitivity analysis. Using the equation of Broecker (1981): $K_v = 3.7·10^{-8}·\delta\rho^{-1}·\delta z$ (with $\delta\rho·\delta z^{-1}$ in kg·m^{-4}), the diffusivities in the bloom in the North Sea varied between $1·10^{-6}$ and $6·10^{-6}$ m^2·s^{-1}. Because the higher diffusivity mentioned above gave virtually the same model output as a diffusivity of 0 these lower values were not used.

In the model all sedimented material is remineralised instantaneously. Since the model results were not very sensitive to diffusion from the deep layer this assumption was not explored any further.

Differential equations

$\mu_{E.hux}$	$= \mu_{max, E.hux}*[NO_3]/([NO_3]+K_{1/2, E.hux})$
μ_{cyano}	$= \mu_{max, cyano}*[NH_4]/([NH_4]+K_{1/2, NH4})$
sedim	$=$ SEDIMENTATION
calcif	$=$ CALCIFICATION
dissolution	$=$ conditional (calcif $> \mu_{max, E.hux}/2$, $diss_{before}$, $diss_{after}$)
$\delta[NO_3]·\delta t^{-1}$	$= -\mu_{E.hux}* POC_{E.hux}/$ cn+DIFN/ mld
$\delta POC_{E.hux}·\delta t^{-1}$	$= \mu_{E.hux}* POC_{E.hux}+$ (-solubilisation –degradation +sedim)* $POC_{E.hux}$
$\delta[POC_{cyano}]·\delta t^{-1}$	$= \mu_{cyano} * [POC_{cyano}]$
$\delta[NH_4]·\delta t^{-1}$	$=$ degradation* $POC_{E.hux}/$ cn- remineralisation* [DOC]/ cn- $[POC_{cyano}]*$ $\mu_{cyano} /$ cnh4

$\delta[DOC]\cdot\delta t^{-1}$	= solubilisation* $POC_{E.hux}$+ remineralisation* [DOC]+DIFDOC/ mld
$\delta[DOCdeep]\cdot\delta t^{-1}$	= -DIFDOC/ dld
$\delta[CaCO_3]\cdot\delta t^{-1}$	= $POC_{E.hux}$*(calcif- loss* (degradation+ solubilisation-sedim))* cp+ dissolution* $[CaCO_3]$+ sedim* $[CaCO_3]$]
$\delta[DIC]\cdot\delta t^{-1}$	= -($\mu_{E.hux}$-degradation)*$POC_{E.hux}$ -($POC_{E.hux}$* (calcif- loss* (degradation+ solubilisation- sedim))*cp+ dissolution* $[CaCO_3]$)- remineralisation* [DOC]+ DIFDIC/ mld+ AIRSEA- $[POC_{cyano}]$* μ_{cyano}
$\delta[alkalinity]\cdot\delta t^{-1}$	= -2*($POC_{E.hux}$* (calcif- loss*(degradation+ solubilisation-sedim))* cp +dissolution* $[CaCO_3]$)+ DIFalk/ mld- $\delta[NO_3]\cdot\delta t^{-1}$* $potAlk_{NO3}$+ $\delta[NH_4]\cdot\delta t^{-1}$* $potAlk_{NH4}$
$\delta[NO_{3deep}]\cdot\delta t^{-1}$	= -sedim* $POC_{E.hux}$/ cn* mld/ dld- DIFN/dld
$\delta[DIC_{deep}]\cdot\delta t^{-1}$	= -sedim* ($POC_{E.hux}$+ $[CaCO_3]$)*mld/ dld- DIFDIC/dld
$\delta[alkalinity_{deep}]\cdot\delta t^{-1}$	= -2* sedim*$[CaCO_3]$* mld/ dld -DIFalk/ dld-$\Delta[N_{deep}]\cdot\delta t^{-1}$* $potAlk_{NO3}$
$[CO_2]$	= CO_2fromDIC,alkalinity
fCO_2	= $[CO_2]/K_0\cdot10^6$

Output [mol·m^{-2}]

air sea flux	= ΣAIRSEA*mld*1000
potential flux	= (ΣAIRSEA +POTFLUX)*mld*1000
sedimented $CaCO_3$	= Σ(sedim* $[CaCO_3]$)*mld*1000
sedimented $POC_{E.hux}$	= Σ(sedim*$POC_{E.hux}$)*mld*1000
DOC	= [DOC]*mld*1000

Rate constants

$\mu_{max, E.hux}$	maximum growth rate *E. huxleyi*	0.69 d^{-1}
$\mu_{max, cyano}$	maximum growth rate cyanobacteria	0.69 d^{-1}
degradation	$POC_{E.hux} \rightarrow$ DIC & alkalinity	0.07 d^{-1}
solubilisation	$POC_{E.hux} \rightarrow$ DOC	0.06 d^{-1}
remineralisation	DOC $\rightarrow$ DIC & alkalinity	0.003 d^{-1}
$diss_{before}$	$CaCO_3 \rightarrow$ DIC & alkalinity	0 d^{-1}
$diss_{after}$		0.17 d^{-1}

Constants

$K_{½, E.hux}$	half-saturation constant *E. huxleyi*	0.1 µM
$K_{½, cyano}$	half-saturation constant cyanobacteria	0.1 µM
cn	C:N ratio $POC_{E.hux}$ and DOC	7.4
cnh_4	C:N ratio cyanobacteria	6.625
cp	calcification:photosynthesis ratio	0.433
loss	$CaCO_3$ loss associated with $POC_{E.hux}$ loss	0.75
$potAlk_{NO3}$	effect of NO_3 and HPO_4^{2-} on alkalinity	1.1396 µeq·µM^{-1}
$potAlk_{NH4}$	effect of NH_4^+ and HPO_4^{2-} on alkalinity	0.875 µeq·µM^{-1}
mld	mixed layer depth	40 m
dld	deep layer depth	80 m
k_{dif}	turbulent diffusion between ml & dl	0.0216 m·d^{-1}
k_{av}	CO_2 gas transfer rate	4.229 m·d^{-1}
delay	delay between calcification and photosynthesis	2 d

Initial concentrations

$POC_{E.hux}$		0.1 µM
$[NO_{3, deep}]$		6 µM

$[DOC] = [POC_{cyano}] = [NH_4]$ 0 µM

$[DIC_{deep}]$ 2157 µM

$[alkalinity_{deep}]$ 2372 µeq·L^{-1}

Functions

DIFx $= k_{dif}* (x_{dld} - x_{mld})$

AIRSEA $= k_{av}* (CO_{2,air} - [CO_2])$

CALCIFICATION $= \mu_{E.hux}(time - delay)$.

         IF time < delay THEN CALCIFICATION $= \mu_{max, E.hux}$

CO_2fromDIC,alkalinity= CO_2 calculated from DIC and alkalinity based on the CO2SYSTM program by Lewis & Wallace (http://cdiac.esd.ornl.gov/oceans/co2rprt.html), using K_1 and K_2 according to Roy et al. (1993) and other dissociation constants as compiled by Millero (1995).

POTFLUX $=$ DICfromAlkalinity$_{potflux}CO_{2,air}$ - DIC$_{potflux}$. Alkalinity$_{potflux}$ and DIC$_{potflux}$ are calculated after mineralisation of all particulate and organic carbon in the mixed layer. DICfromAlkalinity$_{potflux}CO_{2,air}$ works like CO_2fromDICalkalinity.

SEDIMENTATION $= -V_{sink}* 3600* 24/$ mld. The sinking speed (V_{sink}) is calculated from Stokes' law by interpolation of the following equations:

V_{sink} $= (2*V*g*\Delta\rho/ (A*\rho*C_d)^{0.5}$

Re $= V_{sink}*\rho*r/\eta$

C_d $= intercept*Re^{power}$

The relationship between the drag coefficient (C_d) and the Reynolds number (Re) was of the form derived by Aldredge & Gotschalk (1988), and the parameter values are between those for diatom-dominated marine snow ($C_d = 105*Re^{-0.97}$) and other marine snow ($C_d = 95*Re^{-1.87}$, Alldredge & Gotschalk 1988). In the model intercept = 100. In the sensitivity analysis the value of power is varied to obtain sedimentation rates that were comparable to those obtained by using fixed rates of sedimentation between 0.02 and 0.12 d^{-1} (Wal et al. 1995). V, A and r are the volume, area, and radius of the fecal pellets that constituted the main part of the sedimented material during the North Sea bloom (see Wal et al 1995 for details on the collection of samples). $V = 3·10^{-13}$ m^3, $A = 2.14·10^{-9}$ m^2 and $r = 4.153·10^{-5}$ m. ρ is the density of seawater= 1.0267 kg·L^{-1}. g is the gravitational constant= 9.8 m·s^{-2}. η is the kinematic viscosity = 1 g·m^{-1}·s^{-1}. The excess density of the sedimented material ($\Delta\rho = (M_{E.hux}* POC_{E.hux}+ 100*[CaCO_3])/ (M_{E.hux}*POC_{E.hux}/ \rho_{org}+ 100* [CaCO_3]/ \rho_{CaCO3})- \rho$) was calculated from the effective densities of $CaCO_3$ and $POC_{E.hux}$ in the ratio of their standing stocks. $M_{E.hux}$ was estimated as 240 g·mol^{-1}, since carbon is about 5% of wet biomass. ρ_{org} was estimated as 1.027 kg·L^{-1}. $\rho_{CaCO3} = 1.66$ kg·L^{-1} was estimated from the density of calcite (2.8 kg·L^{-1}) and the amount of water included in the coccosphere, which was estimated from the cell radius with and without coccosphere (Bleijswijk et al. 1994b) and the amount of $CaCO_3$ per coccosphere (Bleijswijk et al. 1991). There was no sedimentation of $CaCO_3$ when $POC_{E.hux}$ became 0 µM.

BOFS North Atlantic pCO$_2$ data

     Data of the two cruises with the RRS Charles Darwin (CD60 and CD61) were retrieved from the CD-ROM (Lowry et al. 1994) of the biogeochemical ocean flux study (BOFS). The reported pCO_2 was converted to fCO_2 (Weiss 1974).

Results

Model output

     The development of the bloom is characterised by four successive stages:
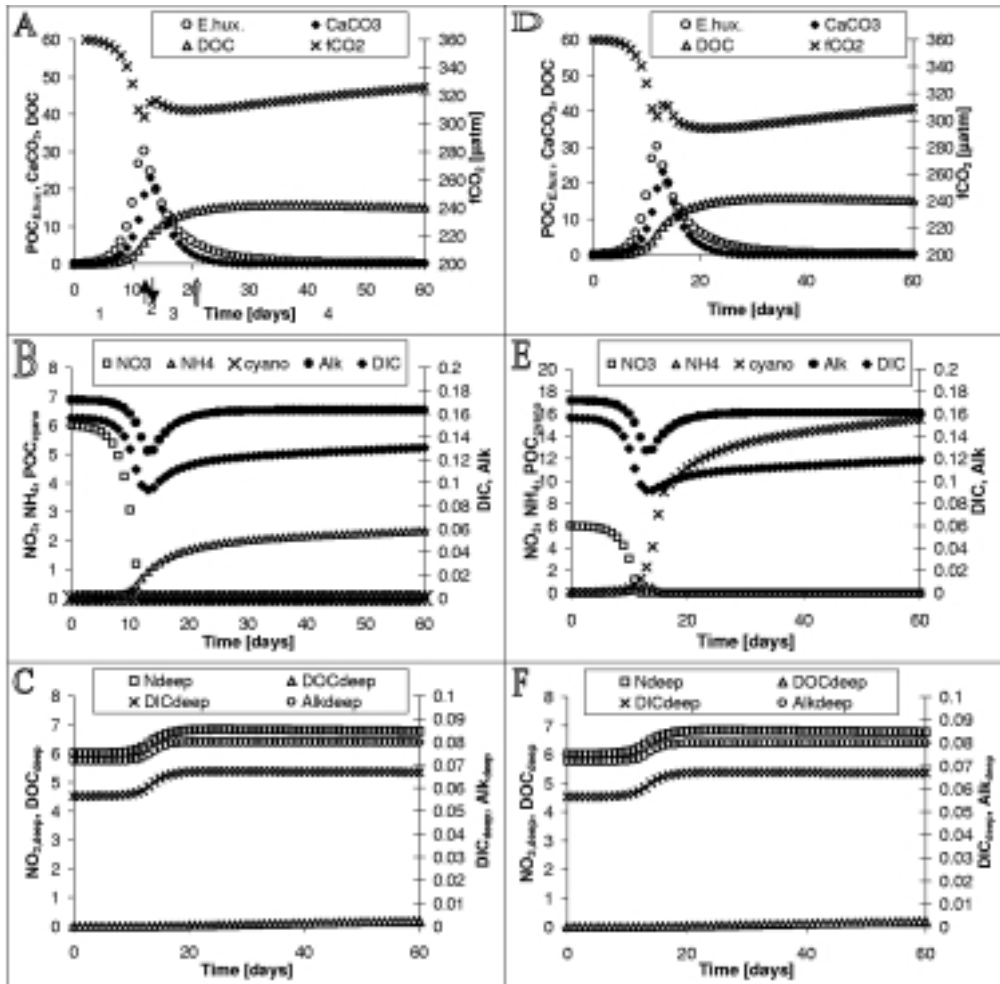
Figure 5.2 a-c) Results of the standard run. d-f) Results including POC_{cyano} using ammonia (NH_4). The successive stages of the bloom marked 1 to 4 are explained in the text. $\uparrow$ $POC_{E.hux}$ maximum, $\downarrow$ $CaCO_3$ maximum, $\Uparrow$ second fCO_2 minimum. $POC_{E.hux}$, $CaCO_3$, DOC, NO_3, NH_4, POCcyano, $NO_{3,deep}$, DOC_{deep} in µM, DIC [mM –2], Alk [meq/L –2.2], DIC_{deep} [mM –2.1] and Alk_{deep} [meq/L –2.3].

Stage 1) The growth stage lasts as long as the gross growth rate is higher than the loss rate. At this point $POC_{E.hux}$ goes through a maximum, fCO_2 goes through a (local) minimum (Figure 5.2a, d) and nitrate (NO_3^-) is nearly depleted (Figure 5.2b, e). The loss rate is the sum of sedimentation, solubilisation ($POC_{E.hux}$ to DOC) and degradation ($POC_{E.hux}$ to DIC). Degradation and remineralisation (DOC to DIC) release ammonia (Figure 5.2b, e). In the standard model run, which includes only $POC_{E.hux}$ (Figure 5.2a-c), ammonia accumulates (Figure 5.2b), while in the model run which includes cyanobacteria (Figure 5.2d-f), ammonia is used to produce secondary growth of POC_{cyano} (Figure 5.2e).

Stage 2) At the end of the growth stage, when $POC_{E.hux}$ growth becomes nutrient-limited, $CaCO_3$ production continues for another two days, until the dissolution of $CaCO_3$ becomes
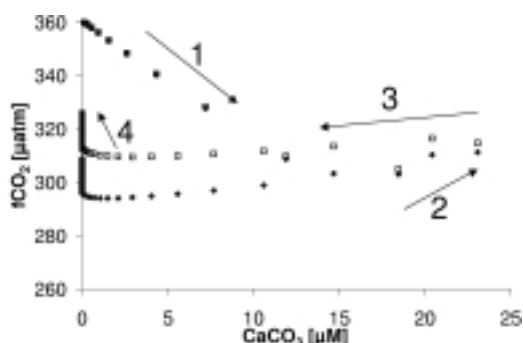
Figure 5.3 The fugacity of CO_2 (fCO_2) as a function of the $CaCO_3$ standing stock. Arrows indicate the direction of time. The successive stages of the bloom, marked 1-4 are the same as in Figure 5.2. □ $POC_{cyano} = 0$ µM as in Figure 5.2a-c, ◆ $POC_{cyano, start} = 0.1$ µM as in Figure 5.2d-f.

higher than its production, and $CaCO_3$ goes through a maximum (Figure 5.2a, d). At this point fCO_2 goes through a (local) maximum. The DOC production rate decreases with the decrease in $POC_{E.hux}$.

Stages 3 & 4) During the declining phase of the bloom $POC_{E.hux}$, $CaCO_3$ and DOC are mineralised. Mineralisation of $POC_{E.hux}$ and DOC increases DIC more than alkalinity. In contrast, dissolution of $CaCO_3$ increases alkalinity more than DIC (Figure 5.2b,e).

Stage 3) During the early part of the declining phase the dominant process is dissolution of $CaCO_3$, and fCO_2 decreases.

Stage 4) During the final stage air-sea exchange of CO_2 and mineralisation of DOC increase the fCO_2. Although depletion of nitrate in the upper mixed layer due to growth (Figure 5.2b, e) and an increase of nitrate in the deep layer by sedimentation (Figure 5.2c, f) create a gradient by which nitrate diffuses upward, this supports only an insignificant amount of $POC_{E.hux}$ during the final stage (Figure 5.2a, d). The ammonia that is produced by remineralisation of DOC gives rise to an increase in POC_{cyano}.

fCO_2 as a function of $CaCO_3$

Figure 5.3 shows fCO_2 as a function of $CaCO_3$. This shows in a different way from Figure 5.2 how the fCO_2 decreases when production of $CaCO_3$ is coupled to production of $POC_{E.hux}$ (stage 1), but increases when production of $CaCO_3$ takes place at the same time as degradation of $POC_{E.hux}$ (stage 2). During the early part of the declining phase the increase in alkalinity outweighs the increase in DIC and therfore fCO2 decreases (stage 3), while in the final stage fCO_2 increases, primarily due to air-sea gas exchange.

Sensitivity analysis

In Table 5.1 and Figure 5.4 a sensitivity analysis is given of the model parameters. Two air-sea CO_2 exchange values are given: a short-term flux that occurs during the bloom and a long term potential flux that is the ultimate effect of the net transport into the deep layer. The short-term flux is the cumulative flux of air-sea exchange during the model run, and thus takes into consideration all processes that sequester carbon, and is dependent on the time that the model is run. The potential flux is the flux after mineralisation of all the particulate and organic carbon in the upper mixed layer and equilibration of the upper mixed layer with the atmosphere. In other words, the potential flux excludes the effect of increased sequestration of carbon (predominantly in DOC and POC_{cyano}) that is degraded in the course of the year, and calculates the effective impact of the net transport of DIC, alkalinity and DOC by sedimentation and diffusion to the deep layer (see the POTFLUX function in Materials & Methods for details).

In the parameters that affect $POC_{E.hux}$ a clear feedback can be seen between degradation, solubilisation and sedimentation (the latter is controlled by the parameter power, see the SEDIMENTATION function in Materials & Methods). If one of these three rates is increased this decreases the amount of $POC_{E.hux}$ that will be passed to the other two processes.

Table 5.1 Sensitivity analysis. PotFlux, potential flux to the deep layer. AirSea, cumulative air-sea gas exchange during the model run. sedCa and sedPOC, cumulative amounts of $CaCO_3$ and POC, sedimented to the deep layer. DOC amount of DOC in the upper mixed layer at the end of the model run. Output in $mol \cdot m^{-2}$.

Parameter[*]	Value	air-sea flux	potential flux	$CaCO_3$ sedimented	$POC_{E.hux}$ sedimented	DOC
Standard run	[*]	0.29	0.42	0.37	0.51	0.61
Degradation (0.06)	0.03	0.33	0.47	0.38	0.55	0.76
$POC_{E.hux} \rightarrow DIC$	0.12	0.22	0.34	0.35	0.43	0.43
delay (2)	0	0.17	0.45	0.08	0.22	0.74
	3	0.26	0.38	0.57	0.61	0.56
Diffusion (0.0216)	0	0.30	0.41	0.37	0.50	0.60
	0.216	0.20	0.43	0.37	0.52	0.67
Dissolution (0/0.17)	0/0	0.18	0.34	0.84	0.70	0.51
$CaCO_3 \rightarrow DIC$	0.17/0.17	0.26	0.44	0.19	0.36	0.67
loss (0.75)	0.44	0.30	0.40	0.48	0.58	0.57
$POC_{cyano, start}$ (0)	0.1	0.29	0.56	0.37	0.51	0.61
NO_3 (6 µM)	10 µM	0.48	0.65	0.62	0.85	1.01
power (-1.2)	-1.08	0.54	0.42	0.51	0.82	0.46
	-1.32	0.10	0.42	0.17	0.21	0.74
remineralisation (0.003) $DOC \rightarrow DIC$	0.03	0.28	0.34	0.37	0.51	0.19
solubilisation (0.07)	0.03	0.34	0.37	0.38	0.56	0.36
$POC_{E.hux} \rightarrow DOC$	0.14	0.22	0.45	0.34	0.42	0.83

[*]values for standard run in parentheses. For dissolution the two values designate the rates before and after the peak of $POC_{e.hux}$.
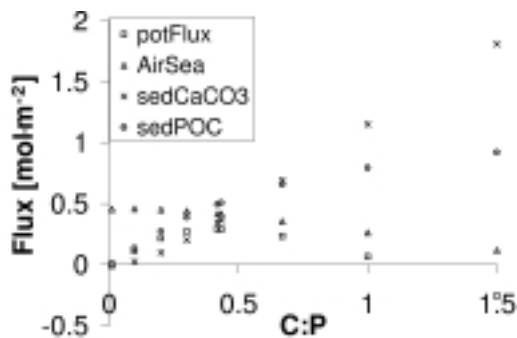

Figure 5.4 Fluxes in the modelled bloom as a function of the C:P ratio of the nitrate-using phytoplankton ($POC_{E.hux}$ box). Ammonia is not used ($POC_{cyano} = 0$ µM). PotFlux is the flux of CO_2 from the atmosphere due to transport of DIC, alkalinity, DOC and NO_3^- to the deep layer. AirSea is the flux of CO_2 from the atmosphere during the model run (60 days). SedCaCO3 and sedPOC are the amounts of $CaCO_3$ and $POC_{e.hux}$ that are sedimented to the deep layer during the model run. Please note that the C:P parameter on the x-axis is not the C:P producion ratio, as is explained in the Materials and Methods section.
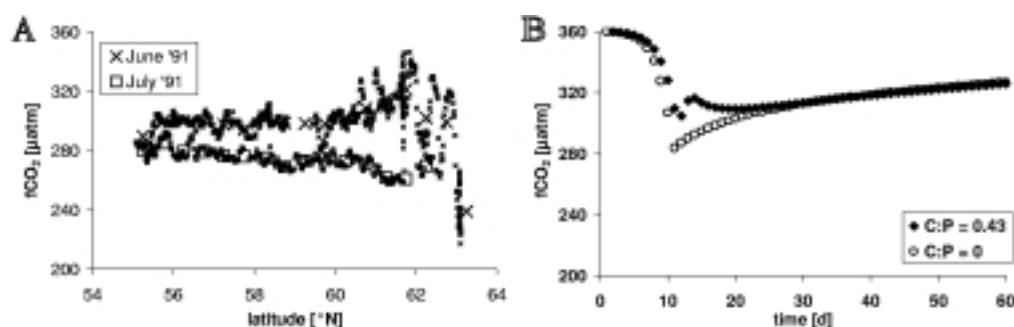
Figure 5.5 a) fCO$_2$ along the 20°W meridian. × Transect from 16 – 21 June 1991 during a bloom of *Emiliania huxleyi*. Transect was sampled from South to North. □ Transect from 24 – 26 July 1991. Transect was sampled from North to South. b) Model output of fCO$_2$ for calcifying (◆) and non-calcifying (◇) nitrate-using algae.

In Table 5.1 it can be seen that if the rates of degradation or sedimentation are increased the amount of DOC formed is decreased. Likewise, if the rates of degradation or solubilisation are increased the amount of POC$_{E.hux}$ that is sedimented is decreased. The effect on the amount of POC$_{E.hux}$ that is degraded is not shown.

The parameters that affect DOC have an opposite effect on the potential flux and the air-sea flux because DOC temporarily sequesters carbon in the upper mixed layer. This DOC will be degraded after the end of the bloom, while the fraction of DOC that is transported to the deep layer by turbulent diffusion is rather limited (Figure 5.2c).

The effect of the changes in CaCO$_3$ cycling on the potential flux and the air-sea flux is less straightforward. On the one hand the chemical effect of production of CaCO$_3$ increases fCO$_2$ and thus decreases the air to sea exchange of CO$_2$. On the other hand the physical effect of inclusion of CaCO$_3$ in fecal pellets increases the sedimentation rate and thus increases the air to sea exchange of CO$_2$. The relative importance of these two effects was tested by varying the C:P parameter in the model to simulate a varying proportion of *E. huxleyi* in the nitrate-using phytoplankton or a different C:P production ratio by *E. huxleyi*. Variation of the C:P parameter gives rise to a weak optimum for the air-sea exchange and a sharper optimum for the potential flux (Figure 5.4). The amount of CaCO$_3$ that is sedimented increases quadratically with the C:P parameter, since there is an increase in both the amount of CaCO$_3$ and the fraction of CaCO$_3$ that is sedimented due to the higher density of the sedimented material. The amount of POC that is sedimented increases asymptotically, since the fraction of POC that is sedimented increases to the same extent as CaCO$_3$, but the total amount of POC that is produced from a fixed amount of nitrate stays the same. Thus, the amount of atmospheric CO$_2$ that is drawn down into the sea goes through a maximum. For the short-term flux the maximum lies at a contribution of 23% *E. huxleyi* of the total POC (C:P = 0.1). For the potential flux the maximum lies at a contribution of 97% of the total POC (C:P = 0.42). The difference between these two is primarily caused by the contribution of DOC to the short-term flux: half of the POC that is not sedimented is converted into DOC, and DOC production increases the air-sea flux, but does not affect the potential flux.

Model validation

The model is based on the results of a field expedition in the North Sea in 1993 and a mesocosm study near Bergen, Norway in 1992. In an attempt to verify the validity of the model results with independent data the model output was compared to data from two field

expeditions in the North Atlantic in 1991 that were collected by J. Robertson (Lowry et al. 1994).

In 1991 two cruises with the RRS Charles Darwin took samples along the 20°W meridian. During the first cruise, in June, a bloom of *E. huxleyi* occurred south of Iceland. The results of this cruise are described by Robertson et al. (1994). The 0.5° averages show that fCO_2 was 10 µatm. higher between 61 and 63 °N, where the bloom of *E. huxleyi* was densest, than between 58 and 60 °N (Figure 5.5a). The data between 61 and 63 °N were collected on 20 June, which was in the week when the bloom was at its maximum extent (Robertson et al. 1994). The data of the second cruise were collected one month later. At this time the fCO_2 was 9 µatm. lower in the region where the bloom had been (61 - 63 °N compared to 58 - 60 °N, Figure 5.5a).

For comparison the model output of fCO_2 are shown for the standard model and the model without calcification (C:P = 0). The fCO_2 is 16 µatm. higher in the calcifying bloom during the week after the $CaCO_3$ peak (Figure 5.5b), when blooms are most visible on satellite images due to shedding of coccoliths by *E. huxleyi*. Thirty days after the $CaCO_3$ peak fCO_2 is 0.4 µatm. lower in the calcifying bloom. Thus, the model shows the same trends as the field observations (Figure 5.5a, and Buitenhuis et al. 1996), but with a smaller amplitude.

Discussion
Comparison of the model output to the mesocosm and North Sea blooms

Although the gross $CaCO_3$ production rate of 0.433 is lower than that found for some other strains, it is consistent with the results for strain CH24 (Buitenhuis et al. 1999), which was isolated from the North Sea in 1991 (Bleijswijk et al. 1991). The model outputs are consistent with measurement in the mesocosms of a peak of $CaCO_3$ that is about ¾ of the POC peak (Bleijswijk et al. 1994a) and in the North Sea of an average $CaCO_3$:POC sedimentation ratio of 0.7 (Wal et al. 1995).

Comparing the model results to the carbon fluxes that were estimated directly from measurements in the North Sea bloom (1.3 mol C·m^{-2} for air-to-sea CO_2-exchange, and 2.4 mol C·m^{-2} of sedimentation, Buitenhuis et al. 1996), it can be seen that both the air-sea flux and the sedimented flux in the model are about three times lower. First of all it can be seen from the sensitivity analysis (Table 5.1 and Figure 5.4) that the ranges for the parameter values give a range of model outputs. More importantly, however, there are at least three elements of bias in the model to explain this about threefold difference:

1) the contribution of other organisms to the carbon sink has been purposely ignored in the standard run in order to extract the contribution of *E. huxleyi* alone to the fluxes. The inclusion of a box for the cyanobacteria gives a first approximation of the effect of secondary growth on ammonia, but via microzooplankton some of this carbon will also be grazed by mesozooplankton or otherwise be transported out of the upper mixed layer (Koshikawa et al. 1999).

2) for the same reason the effects of seasonal warming on fCO_2 and of the wind speed on the surface mixed layer depth have been ignored. The finding that there was a very small correlation between $CaCO_3$ standing stock and water temperature in the 1993 North Sea bloom (Buitenhuis et al. 1996) in the presence of salinity stratification (Veldhuis 1993) suggests that the correlation of water reflectance and water temperature as found by Ackleson et al. (1988) may be primarily due to a correlation between high stratification and *E. huxleyi* abundance and not to coccolith reflectance causing warming of the upper mixed layer. The influence of (the variability of) the wind speed on the magnitude of the carbon sink during a bloom depends on the relative importance of three processes with opposing effects: a shallow upper mixed layer during low wind speeds increases light availability for photosynthesis while high wind speeds increase air-sea gas exchange and increasing wind speeds deepen the wind mixed layer and thereby entrain nutrient-rich deep waters (Hannon et al. 2000).

3) The C:N ratio of the dissolved organic matter (DOM) and the heterotrophic bacteria (which are not included in the model) is usually found to be higher than the 7.4 of the DOM or the 6.625 of the cyanobacteria (POM_{cyano}) that is used in the model. This effect was observed as an increase of the particulate POC:PON ratio during the mesocosm bloom (Bleijswijk et al. 1994a). Unfortunately, not enough data are available to include this mechanism in the model.

Another effect of including POC_{cyano} in the model is to further uncouple the dissolution of $CaCO_3$ from the mineralisation of POC. The other mechanism that uncouples these processes is the delay between the peaks of $CaCO_3$ and $POC_{E.hux}$. This uncoupling gives rise to a decrease in fCO_2 during dissolution of $CaCO_3$ (stage 3 in Figure 5.3). By including POC_{cyano} the slope of this part of the plot increases from 0.4 to 0.9 µatm. $fCO_2 \cdot (\mu M \ CaCO_3)^{-1}$. The slope that was found during the North Sea bloom was 3.5 µatm.·μM^{-1}, indicating that $CaCO_3$ dissolution, POC remineralisation and secondary growth were even further uncoupled, as indicated by the inverse trends between $CaCO_3$ and POC in this bloom (Buitenhuis et al. 1996).

Influence of $CaCO_3$ on air-sea exchange of CO_2

Robertson et al. (1994) found an average increase in pCO_2 (a reduction of the sea-to-air gradient) of 15 µatm. in a bloom of *E. huxleyi*. This was shown by comparing samples in which $CaCO_3$ was greater than 18 µM with samples in which $CaCO_3$ was smaller than 5.5 µM. Buitenhuis et al. (1996) found an increase in fCO_2 of 3.5 µatm.·$(\mu M \ CaCO_3)^{-1}$. Wal et al. (1995) found an enhanced sedimentation of both POC and $CaCO_3$ in the latter of these blooms due to the increased density of fecal pellets, loaded with coccoliths, with an inferred increased sinking rate of the fecal pellets. Buitenhuis et al. (1996) noted the inconsistency between this increase in fCO_2 and an enhanced sedimentation, and also calculated a carbon sink of 1.3 mol C·m^{-2} for this bloom. With the described model these data can be reinterpreted into a consistent explanation. This was possible because the model adds a direction of time to the observations that were collected at different locations in the field studies. The results of the model indicate that the correlation between $CaCO_3$ and fCO_2 (stage 3 in Figure 5.3) does not represent an increase in fCO_2 as $CaCO_3$ is produced, but a decrease in fCO_2 as $CaCO_3$ is dissolved. This is consistent with the fact that both field studies were conducted during the end phase of the blooms, that is, when they were visible on satellite images due to light scattering of coccoliths (Robertson et al. 1994, Buitenhuis et al. 1996).

Thus, it cannot be concluded from the field data that there is a negative correlation between the amount of $CaCO_3$ that is produced and the air to sea flux of CO_2. Therefore, we have addressed this question anew with the model, by performing a sensitivity analysis of the short-term and long-term air-sea CO_2 fluxes as a function of the C:P parameter (Figure 5.4). The most significant feature of this correlation is that the air-sea flux is highest at a C:P parameter value greater than 0, in other words, calcification stimulates the air-sea flux up to a certain point, after which it decreases again. The magnitude of the optimum C:P parameter value is subject to our choice of parameters (such as the change in porosity of the fecal pellets by inclusion of $CaCO_3$, which was estimated by an indirect method, see SEDIMENTATION function in Materials & Methods. However, with recent improvements of the sensitivity in chemical analytical methods it should now be possible to derive the correlation between the POC and $CaCO_3$ contents in individual fecal pellets (POC: Ulrich-Rich et al 1998, $CaCO_3$: within the detection range of graphite furnace AAS) and their densities (Urban et al. 1993) and sinking rates (Harris 1994). Together with the degradation rate (Ploug et al. 1999) this would give the correlation between the $CaCO_3$:POC ratio in the water column and sedimentation rate in a more direct way.

The density excess of diatom frustules, like that of coccoliths, is much higher than that of organic material. Therefore it might be expected that the same mechanism that was found in a bloom of *E. huxleyi* (Wal et al. 1995) would function in blooms of diatoms. However, the

results of Urban et al. (1993) indicate that this may not be the case, due to a lower packing index when the dominant food source was diatoms. The density of fecal pellets changed with the diet of the zooplankton, increasing in the order of diatoms, nanoflagellates and a mixed population including coccolithophores.

Implication for paleoreconstruction and effect of enhanced sedimentation on geological time scales

Our results indicate that even at a modest nitrate concentration of 6 μM at the start of the bloom approximately half of the biomass is produced at an fCO_2 that is more than 32 μatm lower than at the start of the bloom. This implies that the paleoreconstruction of Jasper et al. (1994) may underestimate the oversaturation of upwelling water, because their reconstruction of the fCO_2 of upwelled equatorial Pacific waters over the past 225,000 years was based on the $^{13}C/^{12}C$ ratio of alkenones in the sediment that were produced by prymnesiophyte algae (of which *E. huxleyi* is a member). Thus, most of the signal would be produced during periods when algal growth is high and fCO_2 is relatively low. Moreover, this underestimation could have been larger if production during glacial periods would have been higher, so that the glacial to interglacial difference in oversaturation would have been even larger than the presented 50 μatm (Jasper et al. 1994).

When the effect of $CaCO_3$ to stimulate the co-sedimentation of POC is extrapolated to geological time scales, the control of the alkalinity budget of the ocean on the cycling of $CaCO_3$ becomes important. The cycling of $CaCO_3$ is not controlled by production. Rather, export of Ca/ alkalinity from the upper ocean exceeds import, mostly by rivers, and the excess dissolves in the deep sea. The balance between these processes is maintained by the depth of the saturation horizon of calcite (Milliman et al. 1999). Since atmospheric CO_2 is not controlled by $CaCO_3$ production in the surface ocean, we suggest that the effect of $CaCO_3$ to stimulate sedimentation of POC may enhance drawdown of CO_2 from the atmosphere even more clearly on long time scales than the presented model results for a seasonal bloom suggest.

Summary

Integrating an extensive data set on the cycling of carbon within blooms of *Emiliania huxleyi* into a model it was shown how a positive correlation of fCO_2 and $CaCO_3$ within blooms can be consistent with an enhanced carbon sink for coccolithophorid blooms. It was found that the air to sea CO_2 flux as a function of the C:P parameter shows an optimum C:P parameter value. While the exact value of the optimum C:P parameter value is influenced by many assumptions in the model, the basic form of this function is due to three assumptions:

1) there is a positive correlation between the $CaCO_3$:POC standing stock ratio in the medium and in the fecal pellets. In the model this correlation is 1:1 as found by Harris (1994);
2) there is a positive correlation between $CaCO_3$ content of fecal pellets and sinking rate. This is predicted by Stokes´ law;
3) there is a positive correlation between sinking rate and sedimentation rate.

Additionally, a shortage of data was identified in the following areas:

1) the rates of production and degradation of DOC;
2) the degradation of POC to DIC;
3) the role of cyanobacteria in using regenerated ammonia, and maintaining low fCO_2 pressures during the collapse of the blooms of *E. huxleyi*, and the importance of the coupling between the microbial loop and the classical food chain by micro- and mesozooplankton grazing;
4) the importance of changes in the C:N ratio from new production to DOC and bacterial production to increase the carbon sink per unit of nutrient; and
5) the relationship between the $CaCO_3$ content of fecal pellets and the sedimentation rate.

More generally speaking, the processes of production are much better documented than the processes of decline. Rather than claiming to have provided any definitive carbon budget, we hope to have provided some new insights, as a guide towards obtaining a more accurate budget in the future.

Acknowledgements